

Nonlinear Dynamic Susceptibilities at the Spin-Glass Transition of Ag:Mn

Laurent P. Lévy and Andrew T. Ogielski

AT&T Bell Laboratories, Murray Hill, New Jersey 07974

(Received 4 August 1986)

We have measured the ac nonlinear susceptibilities χ'_3 , χ'_5 , and χ'_7 of very dilute Ag:Mn spin-glasses above and below the transition temperature T_g as functions of frequency, temperature, and magnetic field. In the static limit, these quantities display well defined critical singularities at T_g . The nonlinear susceptibilities can be fitted above T_g by powers of frequency with weakly temperature-dependent exponents. While the effective exponents satisfy the relations imposed by static and dynamic scaling, the observed temperature and frequency roundings suggest the presence of additional length scales.

PACS numbers: 75.30.Cr, 64.60.-i, 75.30.Hx, 75.30.Kz

Metallic spin-glasses consist of magnetic impurities diluted in a noble metal (e.g., Mn, $S = \frac{5}{2}$ in Ag). As a result of their positional disorder, their exchange interaction J which is mediated by the conduction electrons is random. Impurities separated by distances $R < 35 \text{ \AA}$ interact more strongly through the preasymptotic corrections¹ to the Ruderman-Kittel-Kasuya-Yosida (RKKY) interaction $\sim \cos(2k_F R)/R^3$. In addition to the exchange forces, the spin-orbit scattering of the conduction electrons by impurities gives rise to a *random* anisotropy D (Dzyaloshinsky-Moriya), measured to be $\sim 9 \times 10^{-2}$ times smaller than the exchange.² The dependence of the susceptibility of these alloys with temperature exhibits a sharp cusp [Fig. 1(b)], which may be associated either with a gradual freezing of the spins or a genuine phase transition. The existence of a true singularity in

the free energy at the spin-glass transition temperature T_g should be manifest in the power-law divergence of all nonlinear magnetic susceptibilities,³ and their observations should be considered as convincing experimental evidence of a phase transition.^{4,5} Dynamical studies have been limited so far to the linear susceptibility.⁶ We report for the first time a complete spectroscopic study of the nonlinear susceptibilities at ultra-low frequencies (from 10^{-3} to 10 Hz) above and below the transition.

In the vicinity of T_g , the nonlinearities are easily detected in the magnetization response $M(\Omega, t) = \sum \{\theta'_k \times \cos(k \Omega t) + \theta''_k \sin(k \Omega t)\}$ to a harmonic magnetic field $h \cos(\Omega t)$ [Fig. 2(a)]. The nonlinear susceptibilities χ_{2n+1} parametrize the expansion of M in odd powers (by virtue of time-reversal invariance) of h .⁷ In general, each amplitude θ_k contains contributions from all suscep-

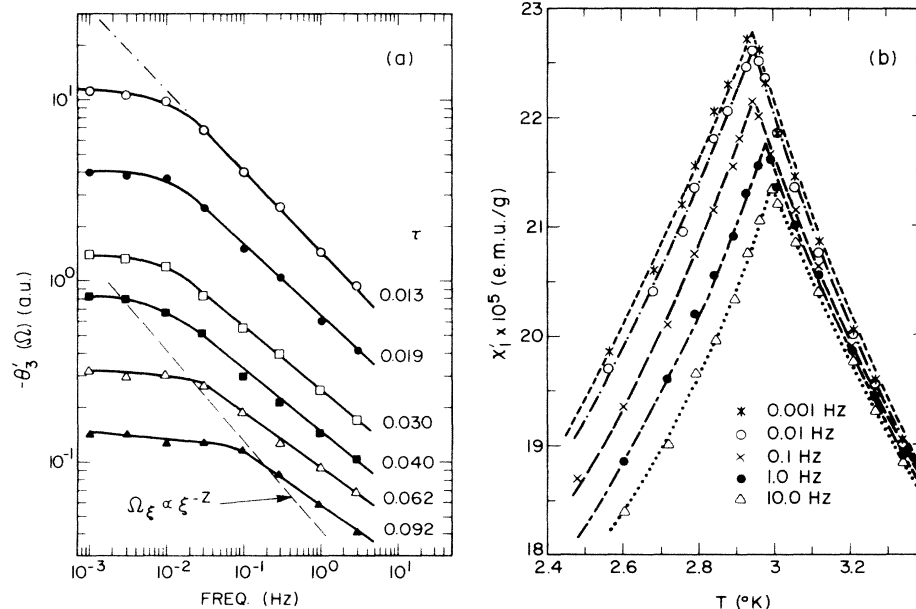


FIG. 1. (a) Frequency dependence of $-\theta'_3 \sim -\chi'_3 h^3/4$ above T_g for several reduced temperatures τ . The slope above 10^{-2} Hz is $-\gamma/(z\nu)$. The dashed line qualitatively shows the shift of Ω_ξ as a function of τ expected from dynamic scaling. (b) Frequency dependence of χ'_1 above and below T_g . Below T_g , the decrease of χ'_1 is nearly logarithmic at frequencies above 10^{-2} Hz.

tibilities $\chi_p, p \geq k$. As the spin-glass transition is approached, χ_5 diverges faster than χ_3 , and θ_3 is no longer proportional to χ_3 . In the absence of a static field, the nonlinear susceptibilities χ'_{2n+1} should be computed in the static limit ($\Omega \rightarrow 0$) by truncating the infinite linear system

$$\begin{aligned} \theta'_1 &= \chi'_1 h + \frac{3}{4} \chi'_3 h^3 + \frac{5}{8} \chi'_5 h^5 + \dots, \\ \theta'_3 &= \frac{1}{4} \chi'_3 h^3 + \frac{5}{16} \chi'_5 h^5 + \dots, \quad \theta'_5 = (\chi'_5/16) h^5 + \dots \end{aligned} \quad (1)$$

at the highest measurable amplitude θ'_{2p+1} .

The time-dependent response $M(\Omega, t)$ is measured with a SQUID (superconducting quantum interference device) susceptometer arranged in an astatic configuration. A small current can be injected in the center of the modulation coil to subtract a constant value from the linear susceptibility. In this way, it is possible to suppress the contribution coming from the linear susceptibility by more than two orders of magnitude. The susceptometer is enclosed in a superconducting tin shield to expel the earth's magnetic field or to trap a static magnetic flux. The samples [Ag:Mn(0.5 at.%) ($T_g = 2.945$ K) and Ag:Mn(0.2 at.%) ($T_g = 1.225$ K)] are mounted on a sapphire rod thermally anchored to a ^3He cryostat, whose temperature is regulated to a part in 10^4 . The SQUID output is synchronously digitized during an integer number of cycles (~ 20). Upon fast Fourier transform, the coefficients θ'_{2n+1} appear as the amplitudes of the peaks in the real part of the spectrum. The presence of the 3rd, 5th, . . . , 11th harmonics in Fig. 2(a) reflects the importance of multispin (at least twelve in this instance) correlations in the vicinity of the transition and signals the divergence of the correlation length $\xi \propto \tau^{-\nu}$, where $\tau = \pm (T - T_g)/T_g$ is the reduced temperature.

At all temperatures above T_g , no significant frequency dependence of the nonlinear susceptibilities is observed below 10^{-2} Hz [Fig. 1(a)]. In this regime we analyze their divergence in terms of static critical exponents. The maximum of χ'_3 which coincides with the maximum of χ'_1 [Fig. 1(b)] at the lowest frequency (10^{-3} Hz) defines T_g . The nonlinear susceptibility χ'_3 reduces in the static limit to the usual spin-glass susceptibility⁸ χ_{SG} and diverges as $\tau^{-\gamma}$. We assume that any temperature (τ) or field ($h - H/T_g$) deviation from the critical point have the same effects on a singular part of the susceptibility when measured on comparable scales, i.e.,

$$M/H - \chi_1 \approx \tau^\beta f(h^2/\tau^\phi) \approx \chi_3 h^2 \tau^{\beta-\phi} + \chi_5 h^4 \tau^{\beta-2\phi} + \chi_7 h^6 \tau^{\beta-3\phi} + \dots, \quad (2)$$

with the exponent $\phi = \beta + \gamma$ and where β measures the growth of the order parameter $q = [\langle S_i \rangle^2]_{\text{av}} \propto \tau^\beta$ below T_g . From Eq. (2), we conclude that χ_5 and χ_7 should diverge as $\tau^{-(\beta+2\gamma)}$ and $\tau^{-(\beta+3\gamma)}$, respectively. Alternatively, $|\chi'_5/\chi'_3|$ and $|\chi'_7/\chi'_3|$ are proportional to $|\chi'_3|^{1+\beta/\gamma}$ in the critical region. This test of scaling is independent of the value of T_g which otherwise enters in the determination of γ . The susceptibilities shown in Fig. 3 were obtained from the amplitudes θ_i measured in the Fourier spectrum [Fig. 2(a)] with use of the procedure outlined in Eq. (1). χ'_3 grows by more than two orders of magnitude in the reduced-temperature range [$10^{-2}, 10^{-1}$] but rounds off within 1% of T_g . From the slope $\log_{10}(\chi'_3)/\log_{10}(\tau)$ in the linear region, we obtain

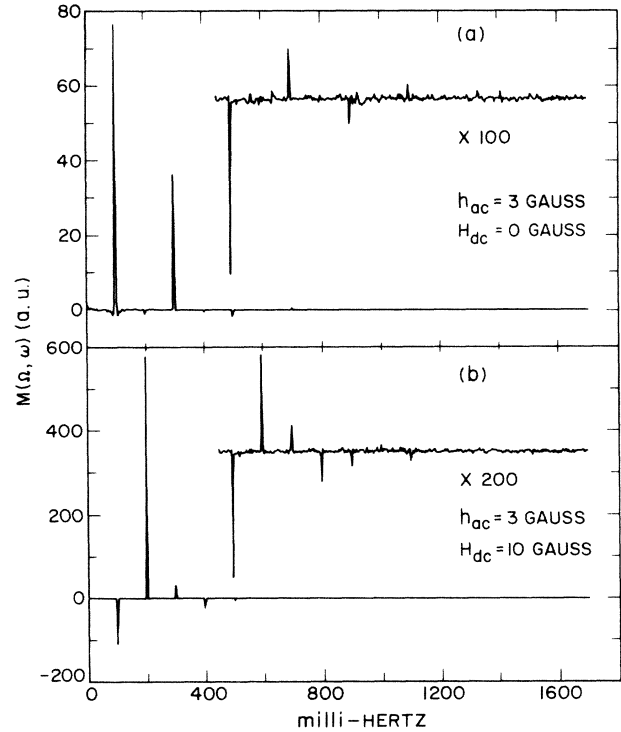


FIG. 2. (a) Fourier-transform spectrum of the magnetization response to a 0.1 Hz field at T_g . The intensity of the fundamental measures the linear susceptibility minus a fixed signal. The resultant amplitude is about -5×10^{-3} of the linear susceptibility. The magnified signal in the upper trace shows the 5th, 7th, 9th, and 11th harmonics. (b) With a static field of 10 G, even harmonics are also observed.

$\gamma = 2.1 \pm 0.1$. This value agrees well with recent measurements performed in low magnetic field,⁵ but disagrees with earlier estimates obtained from the high-field behavior of the susceptibility.⁴ In agreement with the scaling assumption [Eq. (2)], we also find that the ratios $|\chi'_7/\chi'_3|$ and $|\chi'_5/\chi'_3|$ scale as a function of $|\chi'_3|$ with the same exponent $1 + \beta/\gamma = 1.45 \pm 0.1$ (Fig. 3). From this we infer that $\beta = 0.9 \pm 0.2$. The same value of the static critical exponents were found with the 0.2 at. % sample. At T_g , $M/H - \chi_1$ should scale as $H^{2/\delta}$. The exponent δ may be obtained from the scaling relation $\delta = 1 + \gamma/\beta = 3.3 \pm 0.2$. Similarly, the hyperscaling relation $d\nu = 2\beta + \gamma$ gives the critical exponent $\nu = 1.3 \pm 0.2$

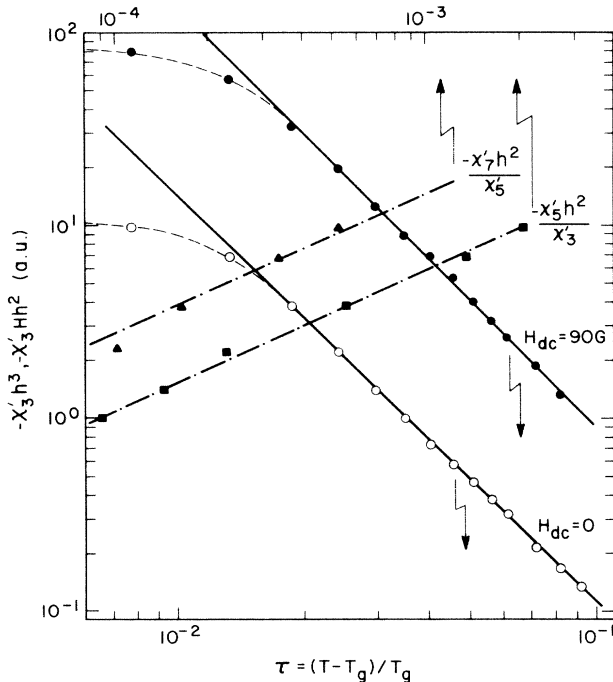


FIG. 3. Temperature dependence of $-\chi'_3$ (vertical axis) above T_g measured at 10^{-2} Hz in static fields of 0 (open circles) and 90 G (solid circles) as a function of reduced temperature τ (lower axis). The slope is $-\gamma$. Plot of the susceptibility ratios $-\chi'_3 h^2 / \chi'_3$, $-\chi'_7 h^2 / \chi'_5$ (top axis) as a function of $-\chi'_3$ (vertical axis) in zero field. The slope is $1 + \beta/\gamma$.

for the correlation length ξ ($d = 3$, the space dimension). If we associate the rounding observed in the nonlinear susceptibilities for $\tau < \tau_r \sim 10^{-2}$ with a cutoff of the correlation length at very long length scales, we estimate the average cutoff length ξ_r from $\xi \approx x l_0 \tau^{-\nu}$, where l_0 is the characteristic distance between impurities and x is a nonuniversal constant found to be of order unity in Monte Carlo simulations of Ising spin-glasses.⁹ For the 0.5 at. % sample, $l_0 = 5.8 \text{ \AA}$.¹⁰ From the divergence of the nonlinear susceptibilities, we conclude that the correlation length ξ is the only relevant length scale in the static behavior, until $\xi = \xi_r$ is of the order of 0.2 \mu m . At this point, the correlation volume contains about 10^8 spins!

In static magnetic fields up to 100 G, the maximum of χ'_3 remains at the same temperature T_g as in zero field whereas the maximum of χ'_1 shifts toward lower temperature. Since the static field H can now interfere with the ac field h , the magnetization response contains even and odd harmonics as shown in Fig. 2(b). With the addition of a static field, an analysis similar to that outlined in Eq. (1) shows that the divergences of χ'_3 and χ'_5 remain well described by the critical exponents measured in zero field (Fig. 3).

Below T_g the nonlinear susceptibilities χ_3, χ_5, χ_7 decrease rapidly with decreasing temperature at all frequencies. At a frequency of 3×10^{-2} Hz, χ'_3 decreases to

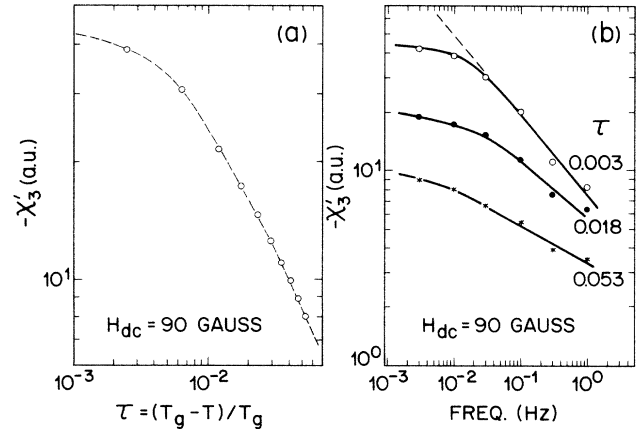


FIG. 4. (a) Temperature dependence of χ'_3 measured at 3×10^{-3} Hz below T_g . (b) Frequency dependence of χ'_3 just below T_g for several reduced temperatures.

a few percent of its critical value at $0.3 \times T_g$, while χ_5 and χ_7 could not be detected. In zero dc field, no static limit could be identified down to 10^{-3} Hz. Above 80 G the frequency dependence softens significantly [Fig. 4(b)] and an analysis in terms of static critical exponents may be possible. From the data shown in Fig. 4(a), we estimate that the effective exponent γ' is close to 2, which is consistent with scaling ($\gamma' = \gamma$).

In a very small ac field and zero dc field, $\theta_3 \propto \chi_3$ ($3\Omega, 2\Omega, \Omega$) measures directly the frequency dependence of χ_3 . At frequencies higher than 10^{-2} Hz, this quantity diverges as a power law of frequency [Fig. 1(a)]. With the assumption that in this range the relaxation time of order parameter, $t^* \propto \tau^{-z\nu}$, is the only relevant time scale (dynamical scaling),¹¹ the nonlinear susceptibilities χ_3 and χ_5 should scale with frequency as

$$\begin{aligned} \chi_3 &\approx \Omega^{-\gamma/z\nu} g_3(\Omega t^*), \\ \chi_5 &\approx \Omega^{-(2\gamma+\beta)/z\nu} g_5(\Omega t^*). \end{aligned} \tag{3}$$

As $T \rightarrow T_g$, the slopes $\log_{10}(\chi'_3)/\log_{10}(\Omega)$ and $\log_{10}(\chi'_5)/\log_{10}(\Omega)$ should therefore approach $-\gamma/(z\nu)$ and $-(2\gamma+\beta)/(z\nu)$, respectively. At frequencies greater than 10^{-2} Hz and close to T_g , their measured values [Fig. 1(a)] 0.30 ± 0.02 and 0.69 ± 0.07 give the same value of the effective exponent $z\nu = 7 \pm 0.6$, in agreement with dynamic scaling. A variation in the slope of $\chi'_3(\Omega)$ with temperature reflects the shape of the scaling function. As long as $\xi < \xi_r$, the relaxation time of a correlated region of size ξ is of order $\Omega \xi^{-1} \approx t_0 (\xi/l_0)^z$, where t_0 is a microscopic relaxation time of the order of $10^{-11} \pm 1$ s. Since frequencies below Ω_ξ probe length scales greater than ξ , the nonlinear susceptibilities should saturate when $\Omega < \Omega_\xi$. This behavior is qualitatively observed in Fig. 1(a) at reduced temperatures greater than 0.05. Although this value is higher than τ_r , the reduced temperature at which the static nonlinear susceptibility

stops growing, it is consistent with a large correlation volume (10^6 – 10^9 spins).

The frequency dependence of χ_3' below T_g is shown in Fig. 4(b). We limited our measurements to the vicinity of T_g because of the severe drifts and aging effects present in the low-temperature phase. Close to T_g , the fit to a power law $\Omega^{-\lambda}$ gives the same value $\lambda \approx 0.30 \pm 0.10$ as above T_g . Although power laws are expected in the critical regime, we also considered logarithmic scaling $[-\log(\Omega t_0)]^{-\mu}$. With the assumption that t_0 is the microscopic time, the exponent μ is $\approx 0.65 \pm 0.1$.

It is instructive to compare the critical exponents of this RKKY spin-glass (presumably of Heisenberg type with weak Dzyaloshinsky-Moriya anisotropy) with those obtained in Monte Carlo simulations of Ising systems⁹ ($\beta=0.5$, $\gamma=2.9$, $\nu=1.3$, $z=6$). z and ν are quite similar, whereas the differences in β and γ seem to be significant. Monte Carlo simulations of isotropic Heisenberg RKKY systems¹² have failed to observe a transition at a nonzero temperature. While simulations assume a $1/R^3$ decay of the RKKY interaction most experiments are in a concentration regime ($> 10^{-4}$) such that the pre-asymptotic part of the interaction is dominant. The *long-range* character of the interaction is then sufficient to provide a transition but not enough for mean field ($\gamma=1$, $\beta=1$) to be valid.¹³

In conclusion, the static and dynamic measurements reveal long-range spin-glass correlations well explained by a phase transition at T_g . The rounding of the transition appears to be associated with a cutoff of the correlation length.

We thank S. Geschwind for many useful suggestions, D. Fisher and D. Huse for their comments on the manuscript, and J. Mock for his very valuable help in

setting up the cryostat.

¹P. M. Levy and Q. Zhang, Phys. Rev. B **33**, 665 (1986).

²N. de Courtenay, H. Bouchiat, H. Hurdequint, and A. Fert, to be published.

³M. Suzuki, Prog. Theor. Phys. **58**, 1151 (1977).

⁴M. Simpson, J. Phys. F **9**, 1377 (1979); S. Chikazawa, Y. Yochunas, and Y. Miyako, J. Phys. Soc. Jpn. **49**, 1276 (1980); B. Barbara, A. P. Malozemoff, and Y. Imry, Phys. Rev. Lett. **47**, 1852 (1981); P. Monod and H. Bouchiat, J. Phys. (Paris), Lett. **43**, L45 (1982); A. Berton, J. Chaussy, J. Odin, R. Rammal, and R. Tournier, J. Phys. (Paris), Lett. **43**, L153 (1982); R. Omari, J. J. Prejean, and J. Souletie, J. Phys. (Paris) **44**, 1069 (1983).

⁵H. Bouchiat, J. Phys. (Paris) **47**, 71 (1986); P. Gandit, private communication.

⁶C. A. M. Mulder, A. J. van Duynveldt, and J. A. Mydosh, Phys. Rev. B **23**, 1384 (1981); N. Bontemps, J. Rajchenbach, R. V. Chamberlin, and R. Orbach, Phys. Rev. B **30**, 6514 (1984); C. Paulsen, J. Hamida, S. J. Williamson, and H. Maletta, J. Appl. Phys. **55**, 1652 (1984); P. Beauvillain, M. Ma-tecki, J. J. Prejean, and J. P. Renard, Europhys. Lett. **2**, 23 (1986).

⁷R. Kubo, J. Phys. Soc. Jpn. **12**, 570 (1957); W. Bernard and H. B. Callen, Rev. Mod. Phys. **31**, 1017 (1959).

⁸J. Chalupa, Solid State Commun. **22**, 315 (1977).

⁹A. T. Ogielski, Phys. Rev. B **32**, 7384 (1985); R. N. Bhatt and A. P. Young, Phys. Rev. Lett. **54**, 924 (1985).

¹⁰ $l_0 = a/(nc^{1/3})$, $a = 4 \text{ \AA}$ is the lattice const, $n = 4$ is the number of Ag atoms per unit cell, $c = 0.005$ is the concentration.

¹¹P. C. Hohenberg and B. I. Halperin, Rev. Mod. Phys. **49**, 435 (1977).

¹²R. Walstedt and L. Walker, Phys. Rev. Lett. **47**, 1624 (1981); A. Chakrabarti and C. Dasgupta, Phys. Rev. Lett. **56**, 1404 (1986).

¹³A. J. Bray, M. A. Moore, and A. P. Young, Phys. Rev. Lett. **56**, 2641 (1986).